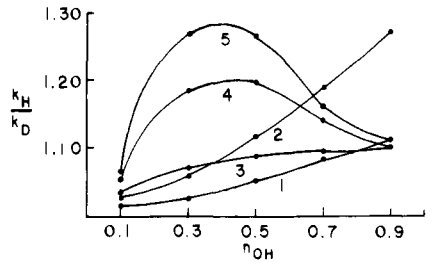

Figure 1. Plot of $(k_H/k_D)_{sec}$ vs. extent of bond formation (n_{OH}) for the reaction $CCHDCH_2Cl + OH^- \rightarrow CCD{=}CH_2 + H_2O + Cl^-$ at 45 °C. Models 1 and 2 include no coupling of C-D bending motions with the C---H stretch. Models 3-5 include increasing extents of such coupling. See text for details.

where $(k_H/k_T)_{sec} > (K_H/K_T)_{sec}$.[7,8]

To explore the possibility of modeling the experimental results, kinetic isotope effect calculations were performed on reaction 2.

$$CCHDCH_2Cl + OH^- \rightarrow CCD{=}CH_2 + Cl^- + H_2O \quad (2)$$

The model is closely similar to those used in earlier calculations,[9] except that the geometry at the α- and β-carbons varies from tetrahedral to trigonal as the HO---H bond order (n_{OH}) varies from 0 to 1. The first set of calculations, (1) and (2), coupled only the O---H, H---C, the H---C,C≡C, and the C≡C, C---Cl stretches by means of off-diagonal F matrix elements, defined as

$$F_{ij} = K(F_{ii}F_{jj})^{1/2} \quad (3)$$

where K is a constant. If $K = A$ for the O---H,C---H coupling and $K = B$ for the C---H,C≡C and C≡C,C---X couplings, then the previously derived[9,10] relationship becomes

$$1 - 2B^2 - A^2 + A^2B^2 = D \quad (4)$$

The curvature parameter, D, controls the magnitude of the imaginary reaction coordinate frequency. The values of A, B, and D were 1.05, 0.33, and -0.20, respectively, as before.[9] If the H---C stretch is also coupled with C-C-D, C≡C-D, and H---C-D bends with $K = C$ in eq. 3, a new relationship between the constants can be derived as before[9,10] and is

$$1 - A^2 - 2B^2 - C^2 + A^2B^2 - B^2C^2 = D \quad (5)$$

To ensure that $F_{st,bd} \rightarrow 0$ for a reactant-like transition state (it must for a product-like one because $F_{C---H} \rightarrow 0$), C was defined as $C'n_{OH}^{1/2}$. Then A and D were assigned constant values while B and C varied with n_{OH}. For models 3-5, the sets of constants used were respectively A, 1.00, 1.00, 1.00, $|C|$,[11] 0.28, 0.49, 0.57, and D, -0.20, -0.30, -0.35. The models thus represent increasingly strong stretch-bend coupling, and increasing barrier curvature. The tunnel corrections were calculated from the $|\nu_L^*|$ values using the first term of the Bell equation.[12]

The calculated $(k_H/k_D)_{sec}$ values at 45 °C as a function of n_{OH} (other reacting bond-order changes concerted with n_{OH}) are shown in Figure 1 for various models. Model 1, in which the bending force constants involving breaking bonds approach a constant value (simulating the sp^3 to sp^2 change) as n_{OH} approaches unity, gives a monotonic increase in k_H/k_D up to a value close to the estimated $(K_H/K_D)_{sec}$. It thus fails to account for cases in which $(k_H/k_D)_{sec}$ exceeds $(K_H/k_D)_{sec}$. Model 2, in which the bending force constants involving breaking bonds approach zero as n_{OH} approaches unity, gives much larger $(k_H/k_D)_{sec}$ values, but the limiting $(k_H/k_D)_{sec}$ as $n_{OH} \rightarrow 1.0$ is ca. 1.3, far larger than $(K_H/K_D)_{sec}$. Neither model gives an appreciable tunnel correction to $(k_H/k_D)_{sec}$.

Table I. Temperature Dependence of $(k_H/k_D)_{sec}$ in the Reaction $CCHDCH_2Cl + OH^- \rightarrow CCD{=}CH_2 + Cl^- + H_2O$

model[a]	n_{OH}	$(k_H/k_D)_{sec,sc}$[b]	$(k_H/k_D)_{sec}$	$\Delta E_a'$[c]	A_H/A_D[c]	$\nu_{LH}^{\ddagger}/\nu_{LD}^{\ddagger}$
1	0.5	1.048	1.053	0.045	0.981	1.002
	0.9	1.113	1.113	0.092	0.963	1.009
2	0.5	1.113	1.117	0.097	0.958	1.002
	0.9	1.272	1.273	0.238	0.913	1.007
3	0.3	1.032	1.069	0.082	0.938	1.019
	0.5	1.058	1.088	0.089	0.945	1.017
4	0.3	1.031	1.184	0.445	0.587	1.037
	0.5	1.056	1.197	0.374	0.663	1.039
5	0.3	1.027	1.270	0.950	0.284	1.041
	0.5	1.052	1.267	0.670	0.440	1.045

[a] See text and legend to Figure 1. [b] The semiclassical (without tunneling) isotope effect at 45 °C. [c] From least-squares fits to Arrhenius equation over the range 25-55 °C.

Models 3-5, on the other hand, do give significant tunnel corrections to $(k_H/k_D)_{sec}$. Models 4 and 5 give $(k_H/k_D)_{sec} > (K_H/K_D)_{sec}$ in the range $n_{OH} = 0.3$-0.7, but in all three models $(k_H/k_D)_{sec}$ approaches $(K_H/K_D)_{sec}$ as $n_{OH} \rightarrow 1.0$. Model 4 most closely matches the experimental results.[7,8] All of these models generate reasonable maximum values (6-9) for $(k_H/k_D)_{prim}$.

Since models 3-5 show little or no relation between $(k_H/k_D)_{sec}$ and the extent of rehybridization ($= n_{OH}$) in the transition state, what does $(k_H/k_D)_{sec}$ reflect? The ν_{LH}^*/ν_{LD}^* values in Table I are clearly largest when $(k_H/k_D)_{sec}$ is largest. Thus $(k_H/k_D)_{sec}$ reflects the extent to which motion of the nontransferred β-hydrogen contributes to the motion along the reaction coordinate.

An experimental criterion for tunneling other than $(k_H/k_D)_{sec} > (K_H/K_D)_{sec}$ is afforded by the temperature dependence of $(k_H/k_D)_{sec}$. Although $A_H/A_D > 0.9$ for models 1 and 2, models 3-5 can generate much smaller A_H/A_D values—around 0.6-0.7 for $(k_H/k_D)_{sec} = 1.20$ and as low as 0.3 for $(k_H/k_D)_{sec} = 1.27$ (Table I). These anomalous Arrhenius parameters should be easy to demonstrate experimentally, and we are currently engaged in such efforts with $(k_H/k_T)_{sec}$ measurements. The isotope effects in the figure and table, incidentally, can be converted to $(k_H/k_T)_{sec}$ by the usual relationship.[6] Agreement with separately calculated $(k_H/k_T)_{sec}$ values is not exact but reasonably close.

Novel Triicosahedral Structure of the Largest Metal Alloy Cluster: $[(Ph_3P)_{12}Au_{13}Ag_{12}Cl_6]^{m+}$

Boon K. Teo* and Kelly Keating

AT&T Bell Laboratories
Murray Hill, New Jersey 07974

Received December 13, 1983

Recently there has been considerable interest in high-nuclearity close-packed metal cluster compounds[1] with metal arrangements resembling fragments of metallic lattices and/or surfaces, particularly in relation to catalysis and surface sciences. We report here preliminary results of the structure of a novel 25-atom cluster containing 13 Au and 12 Ag atoms: $[(Ph_3P)_{12}Au_{13}Ag_{12}Cl_6]^{m+}$ (**1**). This cationic cluster, with the unprecedented geometry of three interpenetrating icosahedra, represents the largest metal alloy (mixed-metal) cluster known to date.

The title compound was prepared by reducing a mixture (Au:Ag = 1:1) of Ph_3PAuCl and $(Ph_3P)_4Ag_4Cl_4$[2] with $NaBH_4$ in ethanol. Synthetic and spectroscopic details will be published separately. The molecular architecture of the cation, as obtained from eth-

(7) Subramanian, Rm.; Saunders, W. H., Jr. *J. Phys. Chem.* **1981**, *85*, 1099-1100.
(8) Subramanian, Rm., unpublished results from these laboratories.
(9) Saunders, W. H. *Chem. Scr.* **1975**, *8*, 27-36; **1976**, *10*, 82-89. Katz, A. M.; Saunders, W. H., Jr. *J. Am. Chem. Soc.* **1969**, *91*, 4469-4472.
(10) Melander, L.; Saunders, W. H., Jr. "Reaction Rates of Isotopic Molecules"; Wiley: New York, 1980; pp 64-66, 75-83.
(11) C' was negative for the first two bends and positive for the last.
(12) Bell, R. P. "The Tunnel Effect in Chemistry"; Chapman and Hall: New York, 1980; pp 60-63.

(1) For reviews, see: (a) Chini, P. *Gazz. Chim. Ital.* **1979**, *109*, 225; (b) *J. Organomet. Chem.* **1980**, *200*, 37, (c) Chini, P., Longoni, G., Albano, V. G. *Adv. Organomet. Chem.* **1976**, *14*, 285; (d) "Transition Metal Clusters"; Johnson, B. F. G., Ed.; Wiley-Interscience: Chichester, 1980.
(2) Teo, B. K.; Calabrese, J. C. *Inorg. Chem.* **1976**, *15*, 2467.

0002-7863/84/1506-2224$01.50/0

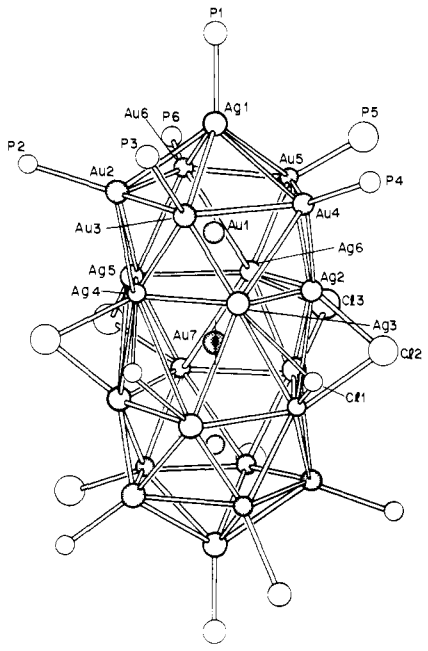

Figure 1. Molecular architecture of the cationic $[(Ph_3P)_{12}Au_{13}Ag_{12}Cl_6]^{m+}$ cluster. The molecule $Au_{13}Ag_{12}$ a crystallographic 2-fold symmetry axis passing through Au7 and the midpoint of Ag3 and Ag3′ or Ag6 and Ag6′ (under *C*2 space group). The symmetry-related atoms, designated as primes, are not labeled for the sake of clarity. Under *C*2/*m* symmetry, the molecule has an additional mirror plane passing through Au7, Au1, Ag1, Ag2, and Au2. In addition, the metal framework has an idealized 5-fold symmetry (along the Au7–Au1–Ag1 axis). All bonds (*12* each) radiated from the encapsulated atoms, Au7, Au1, and Au1′ have been omitted for clarity.

anol/hexane, is portrayed in Figure 1.[3a] A different but isomorphous unit cell was obtained from chloroform/hexane.[3b] The latter gave essentially the same metal arrangement. The metal framework can be described as a cluster containing 10 Au and 12 Ag atoms occupying corners of three interpenetrating triicosahedra and three Au atoms completely encapsulated within the three icosahedral cages. Under *C*2 space group,[3] the molecule has a crystallographic 2-fold axis passing through Au7 and the midpoint of Ag3 and Ag3′ or Ag6 and Ag6′ (the prime designates the symmetry-related atoms, which are not labeled in Figure 1 for the sake of clarity). Under *C*2/*m* space group,[3] the molecule has an additional mirror plane passing through Au7, Au1, Ag1, Ag2, and Au2.

There are 12 triphenylphosphine and six chloride ligands. The 12 triphenylphosphine ligands coordinate to 12 peripheral (surface) atoms: 10 Au (Au2–Au6 and Au2′–Au6′) and two Ag (Ag1, Ag1′) atoms in a radial fashion (viz., away from the centered gold atom, Au1). At this stage of structural determination, all six chloride ligands are doubly bridging, connecting the two 2-fold related silver pentagons (Ag2–Ag6 and Ag2′–Ag6′).

(3) Low-temperature (168 ± 1 K) single-crystal X-ray diffraction data were collected at Molecular Structure Corporation, College Station, TX. (a) $[(Ph_3P)_{12}Au_{13}Ag_{12}Cl_6]A_m{\cdot}n$EtOH ($A^- = Cl^-$ etc.): monoclinic *C*2/*m* or *C*2, $a = 36.082$ (10) Å, $b = 16.581$ (10) Å, $c = 19.338$ (11) Å, $\beta = 101.24$ (5)°; $V = 11348.0$ Å^3, and $Z = 2$. Isotropic refinement in the *C*2 space group gave $R_1 = 10.2\%$ for 1703 independent reflections ($2\theta \leq 40°$) with $I > 3\sigma(I)$. The isotropic thermal parameters for the heavy atoms fall within the range of $1.9 \leq B \leq 3.5$ Å^2 (except Au7 which has a *B* value of 4.5 Å^2), indicating that the metal atoms are properly assigned. At this stage of structural determination, not all the anions and the carbon (including the phenyl rings) or oxygen atoms have been located due to marginal crystal quality caused by facile loss of solvent molecules. As a result, the nature and number of the anion(s) as well as the solvent molecule(s) cannot be ascertained. Furthermore, the assignment of the ligand attached to Ag1 should be considered tentative. Attempts to obtain more stable crystals are in progress. (b) $[(Ph_3P)_{12}Au_{13}Ag_{12}Cl_6]A_m{\cdot}n$CHCl$_3$: monoclinic *C*2/*m* or *C*2, $a = 36.546$ (17) Å, $b = 16.641$ (6) Å, $c = 19.638$ (9) Å, $\beta = 98.70$ (4)°, $V = 11805.7$ Å^3, and $Z = 2$ (work in progress).

Table I. Interatomic Distances (Å) with Esd's

Au1–Au2	2.68 (1)	Au7–Ag2	2.86 (1)
Au1–Au3	2.57 (2)	Au7–Ag3	2.86 (2)
Au1–Au4	2.61 (1)	Au7–Ag4	2.77 (2)
Au1–Au5	2.84 (1)	Au7–Ag5	2.98 (2)
Au1–Au6	2.88 (2)	Au7–Ag6	2.89 (2)
Au1–Au7	2.79 (1)	Ag2–Ag3	2.92 (2)
Au1–Ag2	2.81 (2)	Ag2–Ag4′	3.14 (2)
Au1–Ag3	2.86 (2)	Ag2–Ag5′	3.32 (3)
Au1–Ag4	2.77 (2)	Ag2–Ag6	2.96 (2)
Au1–Ag5	3.01 (2)	Ag3–Ag3′	3.31 (3)
Au1–Ag6	2.83 (2)	Ag3–Ag4	2.87 (3)
Au1–Ag1	2.79 (1)	Ag3–Ag4′	3.54 (3)
Au2–Au3	2.99 (2)	Ag4–Ag5	2.94 (2)
Au2–Au6	2.81 (2)	Ag5–Ag6	3.01 (3)
Au2–Ag4	2.81 (2)	Ag5–Ag6′	2.89 (3)
Au2–Ag5	2.97 (2)	Ag6–Ag6′	3.17 (3)
Au2–Ag1	3.03 (1)		
Au3–Au4	3.04 (2)	Ag3–Cl1	2.61 (5)
Au3–Ag3	2.57 (2)	Ag4–Cl1′	2.63 (5)
Au3–Ag4	2.78 (2)	Ag3–Cl1′	3.38 (5)
Au3–Ag1	3.14 (3)	Ag2–Cl2	2.45 (6)
Au4–Au5	2.93 (1)	Ag4–Cl2′	2.77 (5)
Au4–Ag2	2.54 (2)	Ag5–Cl2′	3.27 (5)
Au4–Ag3	3.02 (2)	Ag5–Cl3′	2.67 (6)
Au4–Ag1	3.07 (2)	Ag6–Cl3	2.53 (6)
Au5–Au6	2.87 (2)		
Au5–Ag2	3.23 (2)	Ag1–P1	2.34 (5)
Au5–Ag6	2.85 (2)	Au2–P2	2.30 (4)
Au5–Ag1	2.99 (2)	Au3–P3	2.41 (6)
Au6–Ag5	3.15 (3)	Au4–P4	2.38 (6)
Au6–Ag6	3.26 (2)	Au5–P5	2.32 (7)
Au6–Ag1	2.86 (3)	Au6–P6	2.38 (6)

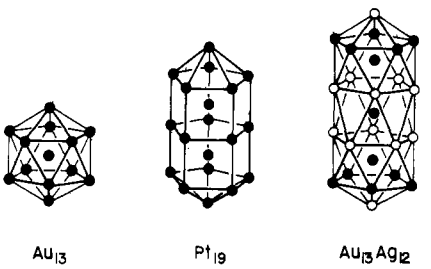

Figure 2. Metal frameworks of the Au_{13} cluster $[Au_{13}(PMe_2Ph)_{10}Cl_2]^{3+}$,[6] the Pt_{19} cluster $[Pt_{19}(CO)_{22}]^{4-}$,[7] and the $Au_{13}Ag_{12}$ cluster $[(Ph_3P)_{12}Au_{13}Ag_{12}Cl_6]^{m+}$ (this work). For the $Au_{13}Ag_{12}$ cluster, the Au and Ag atoms are represented by filled and open circles, respectively. All bonds (*12* each) radiated from the encapsulated atoms have been omitted for clarity.

The interatomic distances are tabulated in Table I. With the exception of two Ag3–Ag4′ distances at 3.54 (3) Å, all metal–metal contacts, ranging from 2.54 (2) to 3.32 (3) Å, can be considered as more or less bonding distances. The metal–metal distances follow the approximate trend of Au–Au < Au–Ag < Ag–Ag.

Under *C*2 space group, the three crystallographically independent chloride ligands are as follows: (1) Cl1 bridges *symmetrically* across Ag3, Ag4′ (Ag–Cl distances of 2.62 (av) Å); (2) Cl3 bridges *symmetrically* across Ag5, Ag6′ (Ag–Cl of 2.60 (av) Å); and (3) Cl2 bridges *asymmetrically* across Ag2, Ag4′ (Ag2–Cl2 of 2.45 (6) Å and Ag4′–Cl2 of 2.77 (5) Å). In addition, close contacts of Ag3′···Cl1 at 3.38 (5) Å and of Ag5′···Cl2 at 3.27 (5) Å are observed, making these ligands semi-triply bridging.

The title compound satisfies the simple electron counting theory we developed recently for high-nuclearity close-packed metal clusters.[4] With three completely *encapsulated* "bulk" and 22 *peripheral* "surface" metal atoms, our theory predicts a total electron count of $3 \times 11.17 + 22 \times 11.17 \times 1.125 = 310$. The observed electron count is 11×25 (metal) $+ 2 \times 12(Ph_3P) + 3 \times 6(Cl) - m = 317 - m$ where *m* is the overall charge of the

(4) Teo, B. K. *J. Chem. Soc., Chem. Commun.* **1983**, 1362.

cation. Conductivity measurements in CH_3CN indicate $m \approx 3$–5 (accuracy limited by solubility). For m = 3 and 5, the cluster will have 4 and 2 electrons over the predicted electron count, respectively. The two longer Ag3–Ag4′ distances of 3.54 (3) Å and the two asymmetric chloride bridges (Cl2 and Cl2′) may be manifestations of the presence of extra electrons. Further work is needed to more accurately determine the charge of the cluster.

In the interpenetrating triicosahedra description, the cation **1** has two *outer* Au-centered Au_7Ag_6 icosahedra and one *inner* Au-centered Au_3Ag_{10} icosahedron. Alternatively, the cluster can be considered as two Au-centered Au_7Ag_6 icosahedra sharing one of the two para vertices (Au7). Yet another description is to recognize that there is an idealized 5-fold symmetry passing through atoms Au7, Au1, and Ag1 such that the cluster can be viewed as having a metal arrangement of 1(Ag):5(Au):1(Au):5-(Ag):1(Au):5(Ag):1(Au):5(Au):1(Ag).[5] In this respect, cluster **1** is related to $[Au_{13}(PMe_2Ph)_{10}Cl_2]^{3+}$[6] and $[Pt_{19}(CO)_{22}]^{4-}$[7] as depicted schematically in Figure 2. Note that the Au_{13} cluster has a metal arrangement of 1:5:1:5:1 whereas the Pt_{19} cluster has a metal disposition of 1:5:1:5:1:5:1. Note also that the adjacent metal pentagons in the cationic Au_{13} and $Au_{13}Ag_{12}$ clusters are staggered with respect to one another, giving rise to *icosahedral* (or *bicapped pentagonal antiprismatic*) *cages* whereas those in the anionic Pt_{19} cluster are eclipsed, giving rise to *bicapped pentagonal prismatic cages*. This can be related to the size of the encapsulated metal atoms with a more positively charged encapsulated atom favoring a smaller icosahedral cage such as that in the gold clusters and a more negatively charged encapsulated atom favoring a larger bicapped pentagonal prismatic cage such as that observed in the platinum cluster.[8]

Recent developments in cluster synthesis[1] have produced high nuclearity metal *clusters* approaching small *crystallites* in *size* and *shape*. In addition to those shown in Figure 2, other structurally known large clusters (largest for each element) are (1) $[Pt_{38}(CO)_{44}H_2]$,[2-9] which has a truncated ν_3 octahedral structure with 32 surface and six bulk atoms and a fcc arrangement, (2) $[Rh_{22}(CO)_{37}]$,[4-10] which has 21 surface and one bulk atom and a mixed fcc/hcp arrangement, and $[Rh_{22}(CO)_{35}H_{5-q+x}]^{q-}$ (q = 4,5),[11] which has 20 surface and two bulk atoms and a mixed fcc/bcc arrangement, (3) $[Ni_{12}(CO)_{21}H_{4-n}]^{n-}$ (n = 2, 3, 4),[12] which has hcp packing, (4) $[Os_{10}C(CO)_{24}]^{2-}$,[13] which has a carbide-centered tetracapped octahedral structure, and (5) $[Ru_{10}C_2(CO)_{24}]^{2-}$,[14] which has an edge-sharing bioctahedral geometry (with two carbides). Also worth mentioning are the following large mixed-metal clusters: the hexacapped octahedral $[Fe_6Pd_6(CO)_{24}H]^{3-}$[15] and the twinned cuboctahedral (hcp) $[Pt_nRh_{13-n}(CO)_{24}]^{(5-n)-}$ (n = 1,2).[16] The latter clusters have 12 surface and one bulk (platinum) atoms. The structures of these high nuclearity metal clusters provide evidence for various *crystal growth pathways*. In this respect, phosphine–coinage metal cluster compounds are particularly interesting in that various growth patterns have been found: (1) *tetrahedral* growth pattern in clusters containing four, five, or six metal atoms; (2) *octahedral* growth pattern in clusters containing six metal atoms; and (3) *icosahedral* growth pattern in clusters containing 8, 9, 11, and 13 metal atoms.[17] The title compound represents the largest *icosahedral* or *pentagonal* growth known to date for any metal clusters. It is also the largest known metal alloy (mixed metal) cluster.

Acknowledgment. We thank Dr. A. P. Ginsberg and C. R. Sprinkle of Bell Laboratories for assistance in conductivity measurements and Molecular Structure Corporation, College Station, TX, for X-ray data collection.

Registry No. Ag, 7440-22-4; Au, 7440-57-5.

(5) Likewise, the disposition of the 18 ligands (12 triphenylphosphines and six chlorides) around the 25-metal-atom framework can be described as an 1(P):5(P):6(Cl):5(P):1(P) array.

(6) Briant, C. E.; Theobald, B. R. C.; White, J. W.; Bell, L. K.; Mingos, D. M. P.; Welch, A. J., *J. Chem. Soc., Chem. Commun.* **1981**, 201.

(7) Washecheck, D. M.; Wucherer, E. J.; Dahl, L. F.; Ceriotti, A.; Longoni, G.; Manassero, M.; Sansoni, M.; Chini, P. *J. Am. Chem. Soc.* **1979**, *101*, 6110.

(8) Interesting structural changes attributable to the size of the encapsulated atom have also been observed in the series $[Rh_{10}S(CO)_{22}]^{2-}$ (Ciani, G.; Garlaschelli, L.; Sironi, A.; Martinengo, S., *J. Chem. Soc., Chem. Commun.* **1981**, 563) or $[Rh_{10}P(CO)_{22}]^{3-}$ (Vidal, J. L.; Walker, W. E.; Schoening, R. C. *Inorg. Chem.* **1981**, *20*, 238), $[Rh_{10}As(CO)_{22}]^{3-}$ (Vidal, J. L. *Ibid.* **1981**, *20*, 243), and $[Rh_{12}Sb(CO)_{27}]^{3-}$ (Vidal, J. L.; Troup, J. M. *J. Organomet. Chem.*, **1981**, *213*, 351). In the latter cluster, some of the metal–metal contacts are longer than that expected for bonding interactions due to the bulk of the encapsulated antimony atom, thereby resulting in a more open structure.

(9) Ceriotti, A.; Chini, P.; Longoni, G.; Washecheck, D. M.; Murphy, M. A.; Dahl, L. F., unpublished results.

(10) Martinengo, S.; Ciani, G.; Sironi, A. *J. Am. Chem. Soc.* **1980**, *102*, 7564.

(11) Vidal, J. L.; Schoening, R. C.; Troup, J. M. *Inorg. Chem.* **1981**, *20*, 227.

(12) Broach, R. W.; Dahl, L. F.; Longoni, G.; Chini, P.; Schultz, A. J.; Williams, J. M. *Adv. Chem. Ser.* **1978**, *167*, 93.

(13) Jackson, P. F.; Johnson, B. F. G.; Lewis, J.; Nelson, W. J. H.; McPartlin, M. *J. Chem. Soc., Dalton Trans.* **1982**, 2099.

(14) Hayward, C. T.; Shapley, J. R.; Churchill, M. R.; Bueno, C.; Rheingold, A. L. *J. Am. Chem. Soc.* **1982**, *104*, 7347.

(15) Longoni, G.; Manassero, M.; Sansoni, M. *J. Chem. Soc.*, **1980**, *102*, 3242.

(16) Fumagalli, A.; Martinengo, S.; Ciani, G. *J. Chem. Soc., Chem. Commun.* **1983**, 1381.

(17) For reviews of gold phosphine clusters, see, for example: (a) Mingos, D. M. P. *Proc. R. Soc. London, Ser. A* **1982**, *308*, 75: (b) Steggerda, J. J.; Bour, J. J.; van der Velden, J. W. A. *Recl. Trav. Chim. Pays-Bas* **1982**, *101*, 164.

Book Reviews

The Elemental Composition of Human Tissues and Body Fluids. By G. V. Iyengar (Institute for Medicine, Nuclear Research Institute, Julich, Germany), W. E. Kollmer (Division for Nuclear Biology, Organization for Radiation and Environmental Research, Neuherberg, Germany), and H. J. M. Bowen (University of Reading, U.K.). Verlag Chemie, GmbH., Weinheim. 1978. XVIII + 151 pp. $31.40.

This is a compact and slim little book containing a compilation of the values for the elemental composition of healthy adult human tissues and body fluids. Data on carbon, hydrogen, oxygen, and nitrogen (except for erythrocytes, nail, and hair) are not covered in this work. The tables cover the essential mineral and trace elements and also include many elements (silver, lead, etc.) important in toxicology or environmental chemistry. The data base for the compilation is "Chemical Abstracts" (up to 1976) with selected editing of the data by the authors. The book, except for a very brief introduction, consists entirely of tables of body tissues and fluids (48 in all). Each table is subdivided into the elements present, the number of samples used to obtain a mass concentration, the method of analysis, and a literature citation. If a sufficient number of mass citations is available for a particular element, a weighted mean of the data is calculated and an upper and lower limit reported.

This book will be a very useful reference source for scientists (chemical, biological, environmental, nutritional, and medical) interested in the elemental composition of human body tissues and fluids. The tables are very well done and easy to use. Coverage of the literature to 1976 was excellent. The information is summarized in a form that is very useful. Because of the large amount of research done in this area since 1976, the literature citations are now of very limited use. However, the book fills a real need and will be a valuable addition to the bookshelf of a scientist with an interest in this area.

J. George Brushmiller, *University of North Dakota*